MICROSCOPIC FEATURES OF FRACTURES AND CRACK PROPAGATION OF TITANIUM ALLOYS

P. Lehr
Laboratoire Matériaux à Haute Résistance
Ecole Nationale Supérieure de Techniques Avancées
Paris France

Introduction

The aim of this paper is to analyse and interpret some of the main characteristics of the fracture surfaces of β heat treated titanium alloys, tested at room temperature, under cyclic or monotonic loadings.

β processing or β heat treatment offer undeniable advantages over the more conventional α + β counterparts. For example, forging in the supertransus higher plasticity temperature range leads to better shape definition and cost reduction, due to lower press load requirements. Furthermore, with a given power press equipment, it is possible to manufacture parts of larger size [1] [2] [3].

Moreover, a substantial improvement in operational properties, such as plane deformation toughness (K_{IC}), fatigue crack propagation resistance and creep behavior are associated to the typical acicular microstructure resulting from β processing or β annealing [4 to 9]. The very same type of microstructure is found in titanium alloy castings [10] or in the melted zone and the thermally affected zone of welded parts.

From a fundamental point of view, it is interesting to acquire a better understanding of the influence of microstructural morphology on the basic mechanical properties of titanium alloys.

Although the results presented here concern only the more widely used Ti-6Al-4V alloy, the conclusions seem to apply in general to other β processed titanium alloys such as IMI 685, Ti-6Al-2Sn-4Zr-2Mo and Ti 11.

Experimental Procedure

A commercial Ti-6Al-4V alloy was used in this study. The material was received as α + β forged and annealed with a chemical composition expressed in weight percent as follows : Al=5.70 ; V=3.9 ; Fe=0.17 ; C=0.035 ; O=0.100 ; N=0.015 ; H=0.005 .

The alloy was vacuum annealed in the β-phase region (1100° C) during one hour and cooled at a rate of 500° C/hour. Such heat treatment yields a coarse acicular structure, convenient for the metallographic aims of this work.

Fatigue crack propagation tests were conducted on a close loop electrohydraulic machine at room temperature, under constant load amplitude and sinusoidal load time wave form, at a frequency of 30 Hz, with a stress ratio R=0.1. In order to operate in plane strain conditions, 20 mm thickness compact tension specimens were used. Crack propagation was followed by optical observations on the polished lateral surfaces of the specimens with a travelling microscope. Crack growth rates were calculated from crack length versus number of cycles data and correlated to the values of the stress intensity range ΔK. The specimens were pulled apart to failure in tension and then submitted to optical and scanning electron microscope (SEM) examinations, carried out systematically in a stress intensity range ΔK of 15 to 35 MPa$\sqrt{m}$. In particular, simultaneous SEM observations were made of the fracture surface and one of the lateral faces of the specimens, under different tilt angles in order to establish the correlations existing between the crack path geometry, the fracture surface appearance and the microstructural morphology of the alloy.

Results

Crack Path Geometry

The microstructure resulting from the applied heat treatment is acicular (fig.1) and typical of all β-processed or β-heat treated titanium alloys. The prior-β grain boundaries are materialized by a border of primary α phase. Each β grain is subdivided in "packets" or "colonies" of parallely aligned, acicular α platelets of almost identical crystallographic orientation. The mean thickness of the α platelets is about 12 μm. A thin film of retained β phase and intermetallic precipitates of β-stabilizing elements (of little solubility in the α phase) constitute the interfaces between platelets.

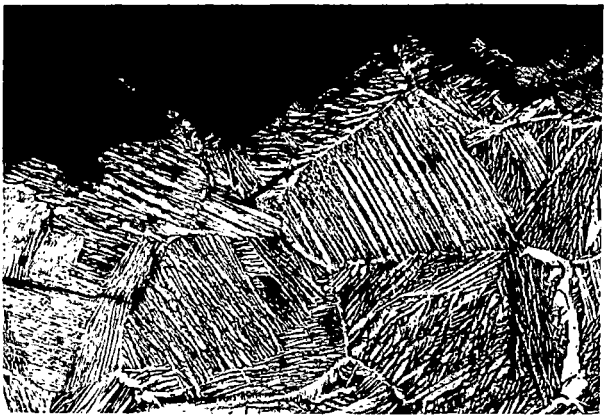

Fig.1 : (optical microscope) Example of fatigue crack path geometry of β annealed Ti-6Al-4V.
$\Delta K = 35.5\ MPa\sqrt{m}$. Magnification 67 times

Fatigue cracks as well as the final fracture propagate through this microstructure in a transgranular manner (fig.1)*. These paths are very tortuous, with frequent changes in propagation direction, heavy crack branching and secondary microcracks formation. The primary α phase borders of the prior-β grains do not constitute a preferential path of propagation.

The tortuosity of the crack path corresponds to a very complex broken relief of the fracture surface, as illustrated by figure 2, taken in the same area as figure 1. In a general way, a close correlation can be established between the fracture path and the microstructural morphology. Changes in the direction of propagation, accompanied or not by secondary microcracks initiation, occur usually at the crossing of the packets boundaries. The size and the crystallographic orientation of the packets appear to be determinant parameters in the control of the fracture surface relief. Moreover, the crack undergoes slight deviations upon crossing from one platelet to another. Figure 3 further illustrates this point showing a secondary crack growing through a prior-β grain from right to left. At first the crack follows the boundaries between adjacent platelets, then it undergoes a break upon entering the next packet located at the center of the micrograph. Here the crack holds the same general direction of propagation but its path is normal to the platelets in-

* For all figures, the general crack propagation directions from right to left.

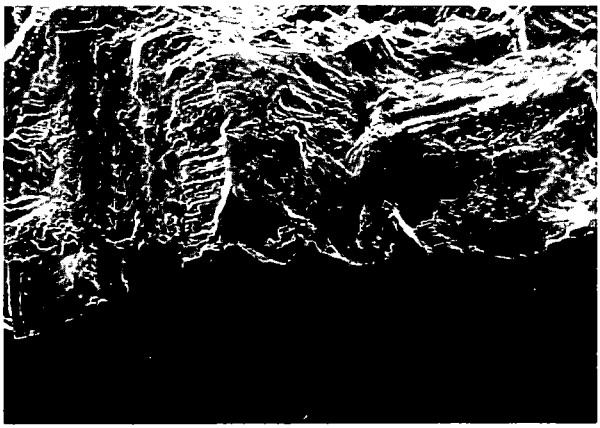

Fig.2 : (SEM). Example of fracture surface appearance of β annealed Ti-6Al-4V. (Specimen tilt angle : 45°. The lateral surface of the specimen appears in black).
ΔK = 34.6 MPa$\sqrt{m}$. Magnification 75 times.

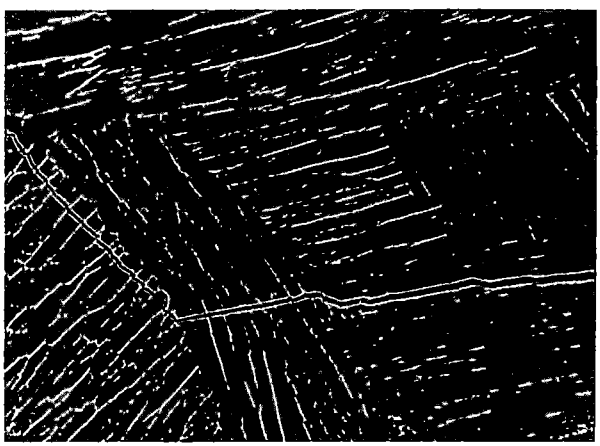

Fig.3 : (SEM). Secondary crack propagating through differently oriented packets of a prior β grain.
ΔK = 36.9 MPa$\sqrt{m}$. Magnification 290 times

terfaces. Later in its way the crack suffers a marked angular deviation when it reaches the packet lying on the left of the figure (which has a different orientation from the previous one) and in which the crack again takes a direction nearly perpendicular to the interplatelets boundaries. Close observation shows small breaks at the platelets interfaces and at certain points the crack follows the boundary between two adjacent packets.

In general fatigue crack growth rates of β-processed or heat treated titanium alloys are lower than those measured on its α + β counterparts, particularly for low ΔK stress intensity range [4] [6] [7] [8] [9]. However more scattering is observed in the fatigue life and crack growth rate data associated with acicular microstructures, where propagation may exhibit a hazardous, unforseeable behavior. Deviations or branching of the main crack lead certainly to a decrease in the growth rate. On the other hand fast propagation may occur when the crack extends in a straight way through conveniently oriented platelets colonies. Therefore it can be considered that the size of packets and their orientation in relation to local stress fields are the chief parameters controlling the kinetics of fatigue crack propagation.

Crack Tip Plastic Deformation

To study this problem from the point of view of crack path geometry, energy balance and the kinetics of fracture propagation the stress relaxation process at crack tip must be taken into account.

According to the usual concepts of fracture mechanics, a plastic deformation occurs in a confined region at crack tip, due to the local stress concentrating effect. Under cyclic loading a monotonic plastic zone is created at each crack opening surrounding a smaller cyclic zone formed at crack closure. An elastic-plastic simple analysis [11] [12] suggests that the diameter r_m of the monotonic plastic zone in plane stress conditions is given by the following expression : $r_m = \frac{1}{6\pi} \left(\frac{K_I}{\sigma_{ys}}\right)^2$ where σ_{ys} is the yield strength of the material and K_I is the crack tip stress intensity factor.

In the present case of β heat treated Ti-6Al-4V alloy the yield strength σ_{ys} is of the order of 830 MPa, which leads to a calculated monotonic plastic zone diameter of 94 μm for a ΔK of 35 MPa$\sqrt{m}$. The macroscopic crack growth rate recorded for such ΔK value is $\frac{da}{dN}$ = 0.58 μm/cycle. Considering the mean platelet thickness (12μm) the preceding result indicates the monotonic plastic zone would extend over nearly eight platelets.

It is obvious this calculation indicates simply an order of magnitude. On the microscopic scale the true plastic zone may differ from the calculated one depending on the effective value of the stress intensity factor and the orientations of both the fracture surface and the crystal lattice in the strained region with relation to the local stress field.

Careful optical microscope examination provides evidence of such plastic deformation as it can be seen in figure 4. On the left side of the figure a concentration of straight slip lines identified as $(10\bar{1}0)$ are observed. On the right hand side the slip lines are closely related to crack growth. These run parallel to the main edge of a step-wise propagating crack.

An important and very often encountered feature is the fact that cracks will frequently grow in straight lines, in a general manner, parallel to the slip traces, indicating the direct crystallographic relationship of this type of preferential fracture path. The upper left part of figure 4 shows the crack propagating, at least partly, along the interfaces between adjacent platelets of the same orientation. Interplatelets boundaries can also play the role of secondary paths for crack propagation.

Moreover it must be pointed out that the slip bands can cross through the whole set of parallel platelets constituting one packet. Such plastic behavior of the packets of platelets is more clearly analysed examining the important plastic zone generated at crack tip when the fatigue cracked specimen was broken in tension. Figure 5, taken in the stretched region at the border of the crack tip plastic zone, shows numerous slip bands extending right through a large colony of platelets of a prior β grain. Thus, from the point of view of

plastic deformation each individual colony behaves as a "quasi-crystal". However it must be observed that the slip bands undergo slight breaks when crossing the interplatelets boundaries and in some instances they even disappear at such points. Hence the interplatelets boundaries can act as obstacles to the motion of dislocations, to the extension of slip bands and, as it will be further demonstrated, to crack propagation.

Fig. 4 : (optical microscope). Slip traces induced by plastic deformation in the vicinity of the fatigue crack. ΔK = 33.9 MPa$\sqrt{m}$. Magnification 290 times.

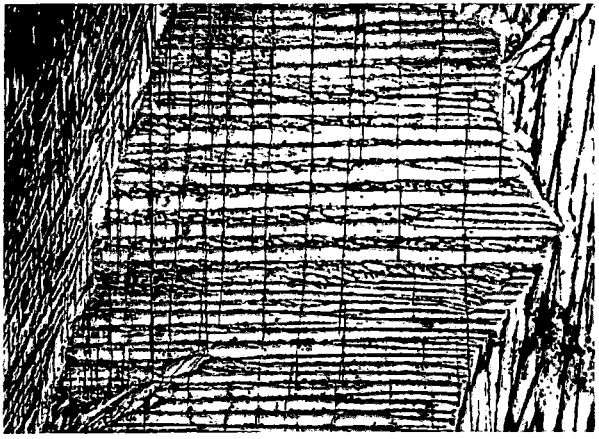

Fig. 5 : (optical microscope). Slip bands extending across a colony, observed in the final fracture stretched zone. Magnification 170 times.

Fracture Surface Appearance

Although fracture surface appearance of β treated titanium alloys is always of a very complex nature, some basic characteristics can be inferred. As it was said, cracks frequently tend to propagate through a given packet in a straight line parallel to plastic deformation slip bands. The fracture surface in this case is rather flat and has a crystallographic meaning analogous to cleavage. An example of such "cleavage type" of surface is given by the SEM fractograph in figure 6, where the straight border of the fracture surface (upper part of the figure) and the side of the specimen (lower part of the figure) are seen. Certain correlations can be established between the fracture surface appearance and the underlying microstructural morphology. In particular the small breakings may be associated to the boundaries between adjacent platelets. A secondary crack with a direction of growth aproximately parallel to the main crack is observed on the lateral surface.

Fig. 6 : (SEM). "Cleavage type" fracture surface appearance (Specimen tilt angle : 45° - The lateral surface of the specimen on the lower part of the figure). ΔK = 35.5 MPa$\sqrt{m}$. Magnification 800 times.

Another good example of "cleavage type" fracture surface is given by figure 7. Here cracking took place in several parallel planes on a step-like arrangement with an orientation aligned close to the general crack growth direction. Figure 8 shows a very demonstrative case of the micro-relief exhibited by "cleavage type" fracture surfaces. In this case the crossing of platelets interfaces, which seemingly again act as barriers to crack propagation, are marked by small wave-like steps on the surface (appearing in white on the fractograph). Other relief features detected run in a sort of divergent traces analogous to cleavage river-patterns, extending in a direction almost perpendicular to the above mentioned platelets interfaces. This same detail can be observed in figure 7.

Fig. 7 : (SEM). "Cleavage type" fracture propagating on various parallel planes.
ΔK = 29.1 MPa$\sqrt{m}$. Magnification 800 times.

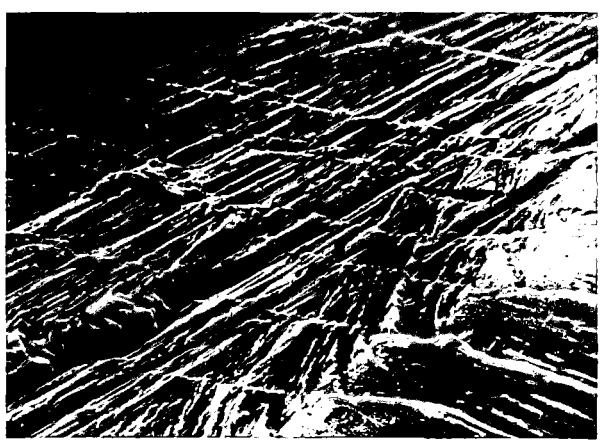

Fig. 8 : (SEM) Example of microrelief exhibited by "cleavage type" fracture surface. (The small steps appearing in white correspond to the intersections of platelets interfaces by the crack surface).
ΔK = 15.3 MPa$\sqrt{m}$. Magnifications 1770 times.

On the other hand, figure 9 taken in the same neighbourhood of figure 7, illustrates a case where the fracture of the sample took place not in a cleavage type of manner but along the boundaries between platelets. Among the secondary inter-platelets microcracks that can be detected one of them is clearly emerging on the lateral surface. Once more the close correlation between the broken morphology of the fracture surface and the platelets disposition on the side of the specimen is observed.

Fig. 9 : (SEM) Example of correlations between the fracture surface appearance and the platelets disposition on the lateral surface of the specimen (lower part of the figure). (specimen tilt angle 45°)
ΔK = 29 MPa$\sqrt{m}$. Magnification 800 times.

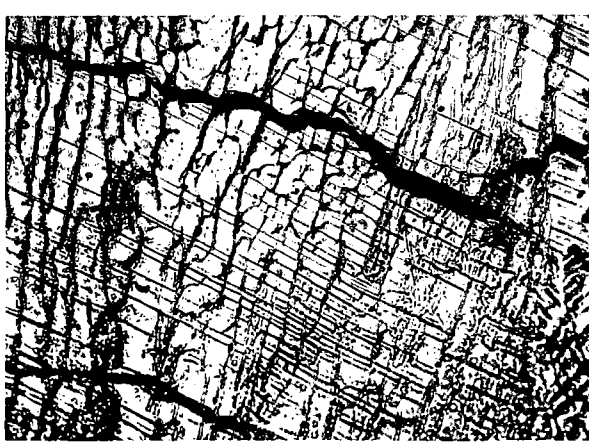

Fig. 10 : (optical microscope) Slip bands and microcracks formation, induced by the final fracture of the specimen. Magnification 400 times.

The morphological characteristics established in the case of fatigue crack growth are also valid for the final rupture propagation when the specimen is pulled apart in tension. Even if the fracture surface appearance of the static failure zone is generally more ductile, recognized by the dimple type of tearings, it seems that the same microstructural parameters control the fracture path. The ultimate separation brings along an important plastic deformation at crack tip, in an area involving several prior β grains. This deformation takes place mainly by prismatic slip as illustrated by figure 10. Furthermore, numerous independent microcracks initiate inside of each colony of platelets, extending by segments parallel to slip traces, but eventually deviating upon crossing of the platelets interfaces. This micrograph emphasizes the important contribution of "cleavage type" fracture to the failure mechanisms of titanium alloys.

Discussion and Conclusions

Solid mechanics suggests a certain number of criteria which allow to forcast the theoretical crack path, under a given loading [13] [14] [15]. For example, according to one of them the fracture path must follow the direction in which the normal stress is maximum. Another one assures that the crack will extend along a path for which the strain energy release rate G is maximum.

In the case of the simple loading mode, to which a compact tension specimen is submitted, these different criteria lead to the same result. The crack will propagate in a plane perpendicular to the applied tensile force.

In fact, the metallographic investigation showed that the fracture surface of acicular type structures is characterized by a broken relief and that a close correlation can be established between the fracture path geometry and the acicular morphology of the microstructure. Interactions between the crack extension and the orientation of the packets of parallely aligned platelets promote frequent changes in propagation direction, numerous crack branching and secondary cracks initiation. All these events are energy consumming. In other respects, a crack inclined with respect to the stress axis is subject to a combination of mode I and mode II type of loadings.

Crack branching and secondary crack extension result in an increase of the specimen's compliance and accordingly in a lowering of the effective stress intensity factor (or of the strain energy release rate) at the main crack tip. These considerations explain that the observed macroscopic crack growth rates (crack extension projected on a single plane normal to the applied stress axis) are generally lower (and more scattered) than those observed for equiaxed structures, for identical values of the stress intensity range ΔK.

On the other hand, this microscop investigation has shown that easy paths of crack propagation exist. The energy consumption during crack extension will be minimized if such paths are characterized by a lower specific fracture energy, or if the associated plastic deformation in the crack vicinity is limited. An important feature is that fracture tends to propagate preferentially through a given packet of parallely aligned platelets following crystallographic planes (most likely prismatic planes). This form of propagation leads to a "cleavage type" of fracture that exhibits a brittle appearance. Another mode of cracking, but seemingly less important, is associated to separation along α platelets interfaces or boundaries of packets of platelets. In these cases the fracture surface appearance is more ductile.

It seems that these observations made in the case of β treated Ti-6Al-4V can be generalized to other β worked or β treated titanium alloys. In an investigation of the low cycle fatigue behavior of processed IMI685, a near α titanium alloy, Eylon, Hall and Schechtman [16] [17] have shown that fatigue crack initiation and the propagation series of events are strongly related to the occurence of slip, with cracking taking place on or parallel to the intense slip bands created during fatigue. Such relationship between slip and fatigue

fracture was also observed in the Ti-11 alloy (Ti-6Al-2Sn .5Zr-1Mo-0.1Si), another near α titanium alloy, with similar microstructure [4] [17]

In conclusion, the fracture propagation path in β treated titanium alloys results from a compromise state between the influence of mechanical parameters (local stress state, strain energy release rate) and microstructural factors (preferential, less energy consuming paths of propagation).

References

1. J. V. Scanlan and G. J. Chambers : *The Science, Technology and Applications of titanium.* Pergamon Press (1970) p. 79.
2. F. J. Gurney and A. T. Male : *Titanium Science and Technology.* Vol. 1 (1973) 431 Pergamon Press (New-York).
3. D. Eylon, C.M. Pierce and J. A. Hall : *Metals Eng. Quat.* Vol. 16, n° 1 (1976) p. 33.
4. D. Eylon, J. A. Hall, C. M. Pierce, D. L. Ruckle : *Met. Trans.* Vol. 7A (1976) 1817.
5. B. Hadj Sassi and P. Lehr : *Mécanique - Matériaux - Electricité* n° 328-329 (avril - mai 1977) p. 3.
6. B. Hadj Sassi : *Thèse Doctorat ès Sciences Physiques.* Université Paris VI. (1977).
7. B. Hadj Sassi and P. Lehr : *J. Less Common Metals.* 56 (1977) 157.
8. P. Lehr : *J. Less Common Metals.* 69 n° 1 (1980) 3.
9. P. J. Bania and D. Eylon : *Met. Trans.* Vol. 9A (1978) 847
10. J. Bevalot : *Matériaux et Techniques* 53 (mai 1975) 203
11. *La Rupture des Métaux.* Masson and Co Ed. (1972) Paris.
12. G. R. Irwin : *Seventh Sagamore Ordnance Materials Research Conference* (Aug. 1960).
13. F. Erdogan and G. C. Sih : *Journal of Basic Engineering* (Déc. 1963) p. 519.
14. D. Bergez : *Thèse Université Paris VI* (1974)
15. G. C. Sih : *Methods of analysis and solutions of crack problems.* P. Nordhoff (1979)
16. D. Eylon and J. A. Hall : *Met. Trans. 8A* (1977) 981.
17. D. Schechtman and D. Eylon : *Met. Trans. 9A* (1978) 1018.